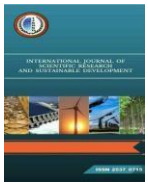

International Journal of Scientific Research and Sustainable Development (IJSRSD)

الاتحاد العربي للتنمية المستدامة والبيئة

Carbon footprint reduction and performance optimization of sustainable free cement concrete with eggshell powder and rice husk ash using machine learning

Mahmoud A. Abdellatief[1], Mohamed Abdellatief[2*], Ezzat Elfadaly[1], and Hassan Hamouda[3]

[1]Evaluation of Nat. Resources Dep., Environmental Studies and Research Institute, University of Sadat City, Egypt

[2]Department of Civil Engineering, Higher Future Institute of Engineering and Technology in Mansoura, Egypt

[3]Civil and Architectural Construction Department, Faculty of Technology and Education, Suez University, Egypt

Article Information

Keywords:

Geopolymer mortar; Eggshell powder; Rice husk ash; Machine learning

***Corresponding author:**

Mohamed Abdellatief

E-mail:

drmohamedabdellatief8@gmail.com

Received: 10/09/2024

Accepted: 10/12/2024

Abstract

This article explores the performance and carbon footprint reduction of geopolymer mortar (GM) that incorporates eggshell powder (ESP) and rice husk ash (RHA) as sustainable alternatives to traditional binders. Using response Surface Methodology (RSM), ESP and RHA were added at volumetric percentages from 0% to 30% as partial replacements for GGBS. The experimental findings revealed that the inclusion of RHA and ESP significantly enhances compressive strength, particularly at optimal dosages, with the highest recorded strength reaching 48 MPa. RSM effectively predicted compressive strength values, aligning well with experimental data. Furthermore, machine learning models, including Gaussian Process Regression (GPR), Artificial Neural Networks (ANN), and Gradient Boosting (GB), were employed to analyze the compressive strength predictions, with GPR demonstrating superior accuracy. An ecological assessment indicated that using RHA and ESP can lower CO_2 emissions compared to traditional materials, thereby promoting more sustainable construction practices. Finally, the dataset of 606 compressive strength results validated the effectiveness of the GPR, ANN, and GB models, all showing high predictive accuracy ($R^2 > 0.85$), with the GPR model outperforming the others.

تقليل البصمة الكربونية وتحسين أداء الخرسانة الأسمنتية الحرة المستدامة باستخدام مسحوق قشر البيض ورماد قشر الأرز باستخدام التعلم الآلي

محمود عبد اللطيف[1]، محمد عبد اللطيف[2]*، عزت الفضالي[1]، حسن حمودة[3]

[1]معهد الدراسات والبحوث البيئية، جامعة مدينة السادات، مصر
[2]معهد المستقبل العالي للهندسة والتكنولوجيا بالمنصورة، مصر
[3]كلية التكنولوجيا والتربية، جامعة السويس، مصر

يدرس هذا المقال الأداء والحد من البصمة الكربونية لملاط الجيوبوليمر (GM) الذي يشتمل على مسحوق قشر البيض (ESP) ورماد قشر الأرز (RHA) كبدائل مستدامة للمواد الرابطة التقليدية. باستخدام منهجية سطح الاستجابة (RSM)، تمت إضافة ESP وRHA بنسب حجمية من 0٪ إلى 30٪ كبدائل جزئية لـ GGBS. كشفت النتائج التجريبية أن إدراج RHA وESP يعزز بشكل كبير من قوة الضغط، وخاصة عند الجرعات المثلى، مع أعلى قوة مسجلة تصل إلى 48 ميجا باسكال. تنبأت RSM بفعالية بقيم قوة الضغط، بما يتماشى جيدًا مع البيانات التجريبية. علاوة على ذلك، تم استخدام نماذج التعلم الآلي، بما في ذلك الانحدار الغاوسي للعملية (GPR) والشبكات العصبية الاصطناعية (ANN) وتعزيز التدرج (GB)، لتحليل تنبؤات قوة الضغط، مع إظهار GPR دقة فائقة. أشار التقييم البيئي إلى أن استخدام RHA وESP يمكن أن يخفض انبعاثات ثاني أكسيد الكربون مقارنة بالمواد التقليدية، وبالتالي تعزيز ممارسات البناء الأكثر استدامة. أثبتت مجموعة البيانات المكونة من 606 نتائج لقوة الضغط فعالية نماذج GPR وANN وGB، حيث أظهرت جميعها دقة تنبؤية عالية ($R^2 > 0.85$)، مع تفوق نموذج GPR على النماذج الأخرى

معلومات عن البحث:

الكلمات الدالة:

الذكاء الاصطناعى، الخلطة الجيوبوليميرية، بودرة قشر البيض، رماد قشر الارز

المؤلف المسئول عن نشر البحث:

محمد عبد اللطيف

الإيميل:

drmohamedabdellatief8@gmail.com

تاريخ الإرسال:

10/09/2024

تاريخ قبول النشر:

10/12/2024

1. INTRODUCTION

Portland cement (PC) significantly contributes to global CO_2 emissions, accounting for about 5–7% of the total emissions, driven by population growth and infrastructure development. This highlights the urgent need for sustainable alternatives due to its high energy consumption and raw material usage alternatives (Abdellatief et al., 2024c; Adamu et al., 2024a; Shah et al., 2021). In response, various high-performance concretes (HPC) have been developed, including PC-based ultra-high-performance concrete (PC-UHPC), known for its compact microstructure, strength, and long-term stability, making it suitable for extreme environments like nuclear waste storage. Recent trends also favor high-performance geopolymer concrete and ultra-high-performance geopolymer concrete as sustainable alternatives (Abdellatief et al., 2024b; Abd Ellatief et al., 2023; Tahwia et al., 2023).

Geopolymer concretes (GPCs) consist of two main components: precursors and an alkaline activated solution (AAS). The precursors, which must contain alumino-silicate, often come from by-product wastes like ground granulated blast-furnace slag (GGBFS) and metakaolin. Several parameters influence the fresh and mechanical performance of GPCs, including the chemical composition, fineness of raw materials, AAS-to-binder ratio, AAS concentration, and curing conditions such as time and temperature (Albidah et al., 2022; Xiao et al., 2020). The composition of precursors plays a crucial role in GPC performance. Lower calcium (Ca) content typically requires higher curing temperatures, while increased Ca levels can reduce setting times and improve strength at lab temperatures. The silica (Si) to alumina (Al) ratio (Si/Al) is also significant; higher ratios generally enhance compressive strength. However, GPC application domains are constrained by this Si/Al ratio, which can be used to classify different GPC types (Abd Ellatief et al., 2023; He et al., 2016; Liu et al., 2022).

Incorporating recycled materials into concrete production can significantly reduce CO_2 emissions. Rice straw and husk are major agricultural wastes, with a global annual output of around 550 million tons. Despite this, their utilization rates remain low, potentially leading to environmental pollution if not managed properly. Many initiatives have aimed to incinerate rice straw and husk for power generation, resulting in substantial quantities of rice husk ash (RHA). However, only a small portion of RHA is currently used as a supplementary material. RHA is primarily composed of silica, found in both amorphous and partially crystalline forms, along with carbon as a major impurity and trace elements like potassium and calcium. Its pozzolanic activity and strong capacity for heavy metal sorption make RHA a promising alternative precursor for adjusting the SiO_2 content in geopolymer concrete. This study focuses on exploring RHA as a sustainable precursor (Hesami et al., 2014; Pandey and Kumar, 2019; Wang et al., 2021). Few studies have explored the use of RHA and eggshell powder (ESP) as precursors in geopolymer concrete, despite the potential benefits of recycling these by-product wastes. Utilizing RHA and ESP not only promotes sustainability in construction but also addresses ecological issues. To the authors' knowledge, there have been no recent investigations specifically focused on RHA and ESP as precursors for geopolymer concrete. This study aims to develop geopolymer concrete using RHA and ESP, examining the extent of the geopolymerization reaction with varying dosages of these materials. Additionally, the research investigates how the content of these waste materials affects porosity, water absorption, and compressive strength. Finally, the CO_2 emissions associated with the produced

geopolymer concrete containing RHA and ESP will be calculated.

2. EXPERIMENTAL PROGRAM

2.1 Materials

The mixtures analyzed in this study were prepared using GGBS, RHA, ESP, natural sand, and superplasticizer.

2.1.1 GGBFS

Ground granulated blast-furnace slag (GGBFS), used as the main precursor, was sourced from an iron factory in Helwan, Egypt. Its specific gravity and fineness were measured at 2.89 g/cm³ and 4.888 g/cm², respectively. The pozzolanic activity indexes of GGBFS were 55.5 at 7 days and 74 at 28 days. X-ray fluorescence (XRF) analysis of GGBFS is presented in Fig. 1.

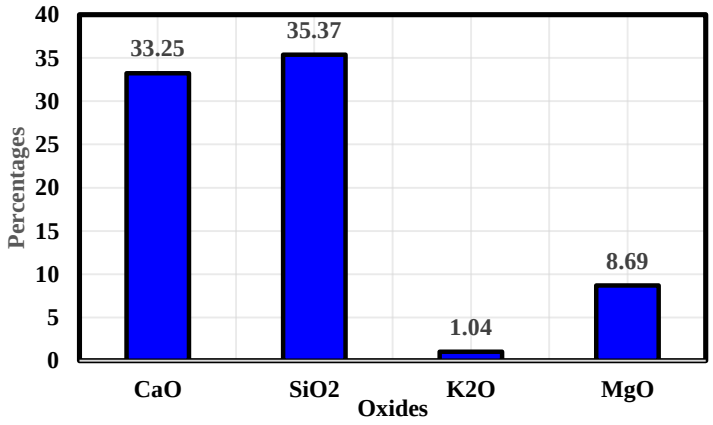

Fig. 1. Oxides of the used materials (wt., %) by XRF

2.1.2 Rice husk ash (RHA)

Rice husk ash (RHA) was produced by incinerating the straw at 600 °C. The resulting ash is dark gray with a specific gravity of 2.17. Chemical analysis of RHA was performed using X-ray fluorescence (XRF), with results summarized in Fig. 2.

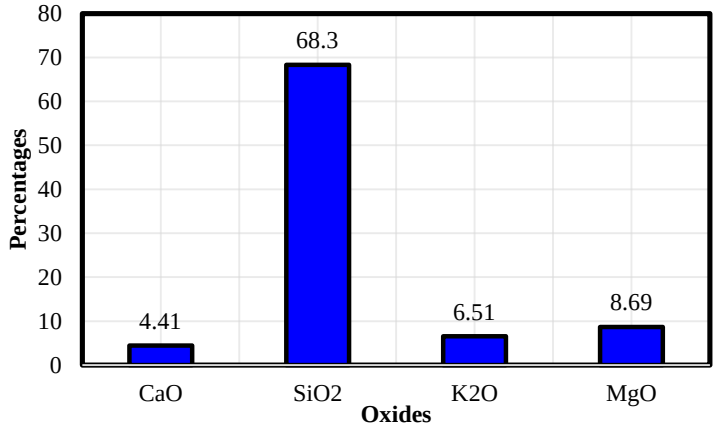

Fig. 2. Oxides of the RHA (wt., %) by XRF

2.1.3 Eggshell powder (ESP)

Eggshell powder (ESP) used in this study has a specific gravity of approximately 2.70 g/cm³ and a surface area that enhances its reactivity. The eggshells were collected, cleaned, and dried before being ground to a fine powder and the major component in its chemical oxides is CaO, as illustrated in Fig. 3.

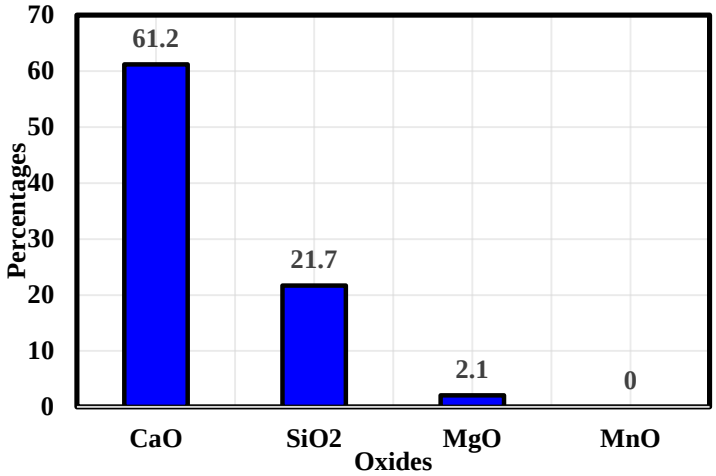

Fig. 3. Oxides of the ESP (wt., %) by XRF

2.1.4 River sand, alkali activation solution, and super-plasticizer

River sand, used as fine aggregate in this study, has a grain size of less than 2 mm, adhering to the C33/C33M Standard Specification for Concrete Aggregates. The water absorption rate of the river sand is 1.02%, and its fineness modulus is 3.03. The alkali activators consisted of a mixture of sodium hydroxide (NH) solution and sodium silicate (SS). A 14 M NaOH solution was prepared and allowed to cool for 24 hours before being combined with SS. The composition of SS is 29.22% SiO_2, 13.66% Na_2O, and 57.12% H_2O (by mass), with a density of 1.39 g/cm³. This mixture was then allowed to mature for one day prior to its use in the geopolymerization process. For this research, Sika ViscoCrete®-3425 Performance Superplasticizer was utilized as a concrete admixture. It complies with the SP standards specified in ASTM C-494 Types G and F, as well as BS EN 934. The density of the superplasticizer is 1.08 ± 0.05 kg/liter, and it has a pH of 4.0.

2.1.5 Mixture proportions

In the current investigation, ten mixtures were formulated to assess the mechanical and durability properties of GM incorporating RHA and ESP, including a control mixture designated as M1. The mixtures involved the substitution of the primary precursor, GGBFS, with RHA at levels of 0% to 30%, and ESP at levels of 0% to 30% using response surface methodology (RSM) (Abdellatief et al., 2023; Cai et al., 2022). Three main variables were addressed to enhance the performance of the GM including ESP content, RHA dosage and SS/NH ratio. The mix proportions of the prepared mixtures are detailed in Table 1.

Table 1. Proportions of the prepared mixtures.

Mixture ID	GGBFS	RHA		ESP	ESP	Sand	SP	SS/NH
	kg/ m^3	%	kg/ m^3	%	kg/ m^3			
M1	700	0	0	0	0	1020	24	2.5
M2	578	0	0	17.5	97	1020	24	1.63
M3	490	0	0	30	167	1020	24	2.5
M4	630	0	0	10	55	1020	24	1
M5	420	30	173	10	55	1020	24	1.03
M6	280	30	173	30	164	1020	24	1.98
M7	490	30	173	0	0	1020	24	2.5
M8	590	15	87	1.0	5	1020	24	1.69
M9	483	15	87	16	89	1020	24	2.47
M10	385	15	87	30	167	1020	24	1

2.2 Techniques for sample preparation

The preparation technique utilized in this investigation was designed to minimize water absorption by the dry compounds to enhance the flowability, as shown in Fig. 4. Initially, the solid materials were dry-blended in the blender for 1.5 min. Subsequently, 50% of AAS and 50% of the SP, were combined and gradually added to the mixer, with mixing continuing for an additional 2.5 mins. In the next phase, the remaining AAS and SP were introduced, and mixing was conducted for an additional 3.0 mins. Once mixture was complete, fresh samples were poured into molds. To enhance compaction and eliminate air bubbles, the molds were placed on a vibrating table after pouring the fresh GM. Previous research has shown that curing geopolymers at elevated temperatures, particularly between 60–80 °C, is one of the most effective methods (Abdellatief et al., 2024a; Adamu et al., 2024b). Therefore, the GM samples were cured in a hot-air furnace at 65 °C for 48 hours before being stored at room temperature until testing (Ahmed M Tahwia et al., 2024; Ahmed M. Tahwia et al., 2024).

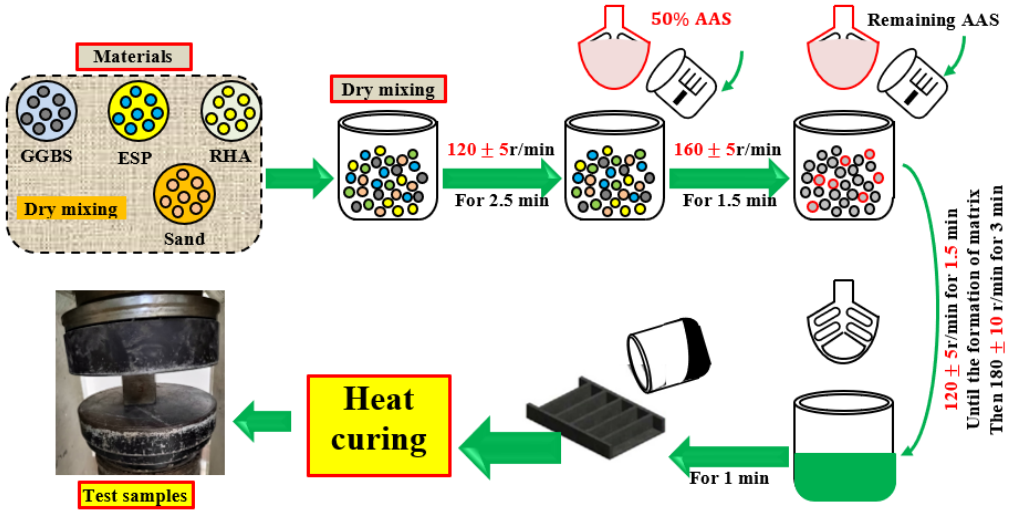

Fig. 5. Preparation process of GM

2.3 Testing methods

The physical, mechanical properties, and durability of the GM mixtures were systematically evaluated in accordance with relevant ASTM standards. The compressive strength (CS) of cubic samples (50 mm × 50 mm × 50 mm) was determined using a standard compression machine with a loading rate of 1.2 kN/s. Recognizing that the strength of ambient-cured geopolymers generally increases with age (Abdellatief et al., 2024a, 2023), tests were conducted at 7 and 28 days to monitor the strength development of the GM. The dry density of the mixtures was evaluated in compliance with ASTM C138/C138M.

2.4 Response surface methodology (RSM)

In the field of scientific and mathematical techniques for optimization, RSM is a frequently utilized approach. To assess the practical relationship between the separate variables and the outcome, a fractional factorial research method is employed. The importance of the developed model is evaluated through the R^2 values, while the influence of specific factors is determined by computing the F-value. A higher F-value indicates that the related parameters have a more significant impact on the study's results (Fig. 5). The group developed numerical models using regression analysis with multiple variables based on findings from experiments on concrete characteristics. The polynomial simulation derived from RSM is represented in Equation 1. The anticipated response value for the established model is denoted by Y, with β_0 serving as the intercept and β_1 and β_2 acting as coefficients for linear effects. Furthermore, β_{11} and β_{22} indicate the parameters for quadratic effects, while β_{12} represents the interaction effect between the variables.

$$y = \beta_0 + \sum \beta_i x_i + \sum \beta_{ii} x_i^2 + \sum \beta_{ij} x_i x_j \quad (1)$$

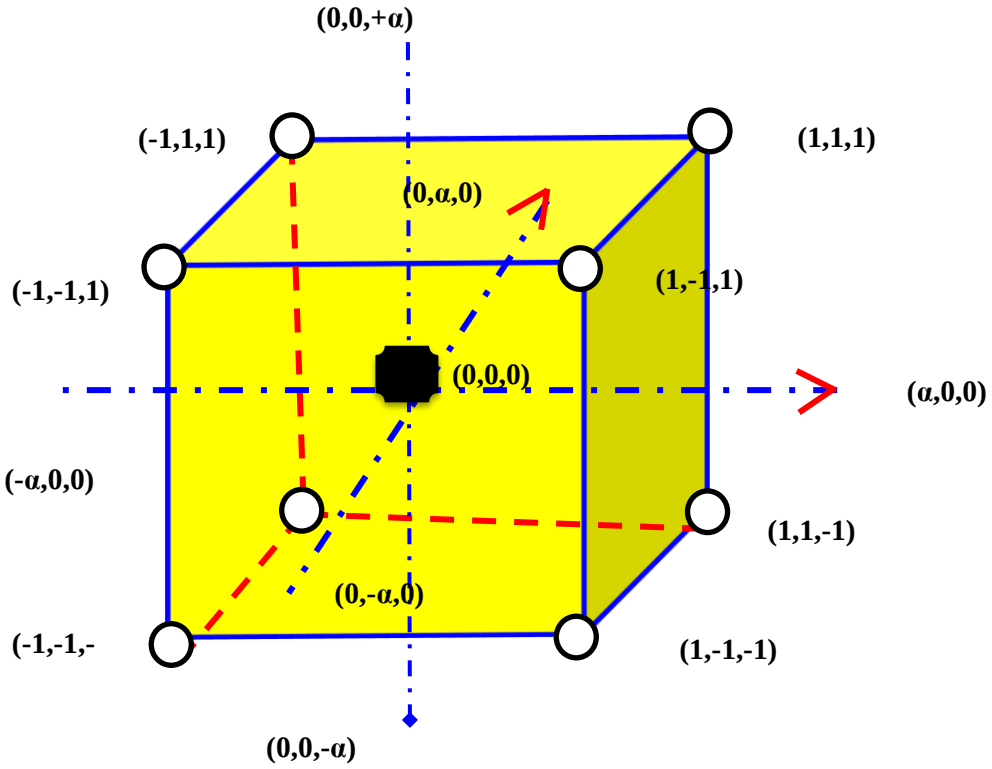

Fig. 5. A visual illustration of CCD

2.5 ML Techniques

ML techniques can be categorized into three groups: supervised, unsupervised, and semi-supervised. In this study, only supervised algorithms were utilized since the objective variable was identified post-data collection. Supervised ML techniques, which use labeled training data for accurate predictions, were employed to derive meaningful insights from the dataset. Specifically, methods like GPR, ANNs, and GB were applied to forecast CS of GM.

2.5.1 Gaussian process model (GPR)

GPR is an effective statistical method for predicting GM based on input parameters. Unlike traditional regression models that rely on fixed functional forms, GPR is a non-parametric approach that models the entire distribution of potential functions. It uses Bayesian inference to combine prior knowledge with observed data, making it adept at handling complex, nonlinear relationships between input and output variables. GPR not only provides point predictions but also generates confidence intervals, helping to assess the reliability of those predictions. Its flexibility allows it to work with various data types, including noisy or sparse datasets common in concrete strength tasks (Abdellatief et al., 2024c).

2.5.2 ANNs (ANNs)

ANNs are a key method in AI, valued for their simplicity, high performance, and low computational needs. Various types exist, including feedforward networks, recurrent networks, and radial basis function networks, all of which analyze relationships between independent and dependent variables. Among these, the multilayer perceptron (MLP) is particularly popular. An MLP comprises an input layer, one or more hidden layers, and an output layer, with

neurons in each layer but no direct connections between neurons of the same layer. The input and output layers have a number of neurons that match their respective variables, while the hidden layer's neuron count can be adjusted for desired outcomes. During training, datasets are inputted to refine the network's weights and biases, minimizing errors by comparing predicted outputs to actual values. MLPs are adaptable, updating their models with new information and effectively representing complex relationships. Their ability to capture nonlinear connections makes them especially effective for predicting concrete strength, improving accuracy across various scenarios (Abdellatief et al., 2024b, 2024c).

2.5.3 Gradient boosting (GB)

Boosting is an ensemble learning technique that transforms a series of weak learners into a strong predictive model. It works by sequentially training learners, where each new model focuses on correcting the errors made by the previous ones. The training data distribution is adjusted based on the performance of each base learner, ensuring that misclassified samples receive more attention in subsequent iterations. Eventually, all weak learners are combined to create a robust final model. GB excels in predicting the CS of GM due to its capability to enhance model performance, manage complex relationships, and deliver precise predictions through ensemble learning (Abdellatief et al., 2024b, 2024c).

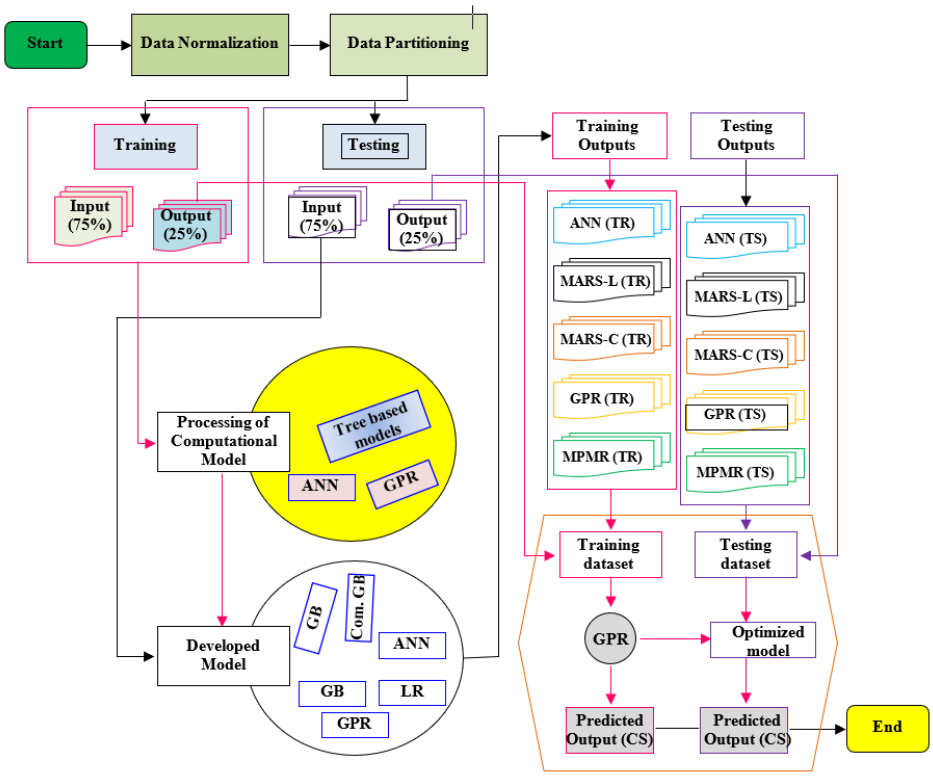

Fig. 6. Schematic view of ML model

2.5.4 Construction of ML models

The prediction process outlined in Figure 4 involves three key steps: data collection, algorithm implementation, and model validation. First, data was gathered based on the chosen input and output variables. This dataset was then split into a training set (75%) and a testing set (25%). The training set was used to create an effective ML model, while the

testing set validated its performance. Figure 5 displays the twelve input features utilized. Three machine learning models—GPR, ANNs, and GB—were developed to predict the CS of GM (Paruthi et al., 2023).

2.5.5 Models Evaluation

To evaluate the models' accuracy, several performance criteria were considered, as outlined below:

$$R^2 = 1 - \frac{\sum_i (y_i - \hat{y}_i)^2}{\sum_i (y_i - \bar{y}_i)^2} \quad (1)$$

$$MAE = \frac{1}{n}\sum_{i=1}^{n} |y_i - \hat{y}_i| \quad (2)$$

$$RMSE = \sqrt{\frac{1}{n}\sum_{i=1}^{n} (y_i - \hat{y}_i)^2} \quad (3)$$

where y_i, $\hat{y}_i$ and $\bar{y}_i$ represent the true, predicted, and average CS results of the GM, respectively.

3. RESULTS AND DISCUSSION

3.1 Dry density

The GM samples were first placed in an electric furnace at a temperature of 100 ºC ±5 ºC for one day to facilitate drying. Afterward, the samples were cooled to reach a temperature of 25 ± 2 ºC. As shown in Fig. 7, the dry densities were measured to assess the impact of waste incorporation. The control mix M1 demonstrated the highest dry density at 2072 kg/m³, while the M6 mixture, which incorporated both types of waste, exhibited the lowest dry density at 1996 kg/m³, marking a reduction of 3.53%. The inclusion of these wastes led to a slight decrease in dry density, attributable to their lower specific gravities. Among the two, ESP had a more significant effect on reducing dry density. The addition of RHA resulted in an approximate 1.88% decrease in dry density, whereas the contribution from ESP was around 1.58%. This difference can be attributed to the specific gravities of RHA and (Abdellatief et al., 2024b; Ifzaznah et al., 2024). as well as the more porous microstructure of samples containing RHA compared to those with ESP, which will be elaborated on further (Hesami et al., 2014; Pandey and Kumar, 2019; Wang et al., 2021).

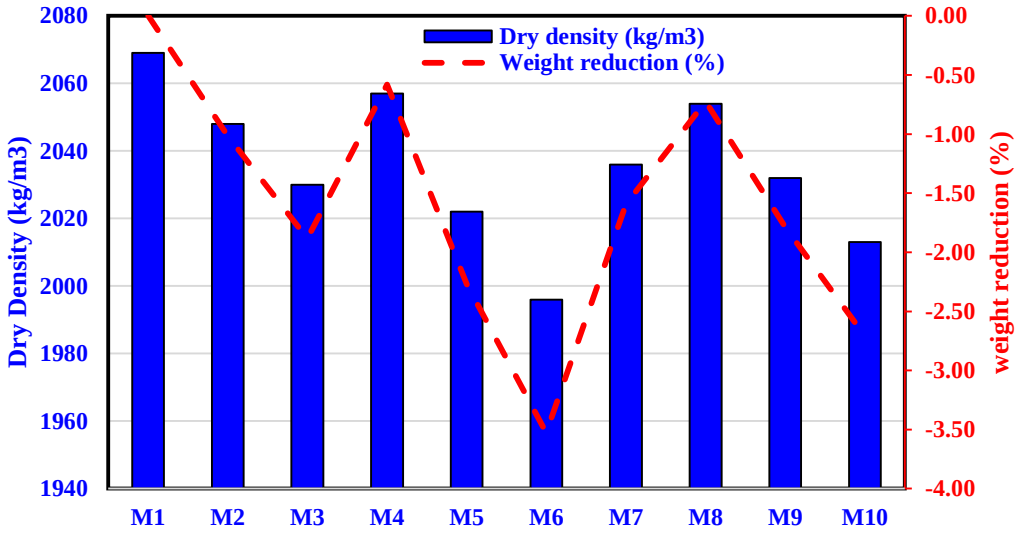

Fig. 7. Variation of dry density in mixes relative to waste replacement ratio

3.2 Response surface for compressive strength (CS)

Fig. 8 illustrates the compressive strength (CS) of the samples in relation to the volume percentages of ESP and RHA. The results indicate that the compressive strength increases with the volume percentage of ESP and RHA (Table 2), peaking at 5% for both materials, particularly with a high SS/NH ratio. The data shows that mixtures with a greater SS/NH ratio exhibit significantly higher compressive strength, achieving a maximum of 1.6. For example, the mixture with a 1.7 SS/NH ratio recorded a compressive strength of 48.0 MPa, compared to the control mix's 38.8 MPa, representing a 23.71% improvement. The highest compressive strength achieved, 48 MPa, resulted from a blend containing 5% RHA and 1.0% ESP at a low level of ESP (around 1%). Furthermore, the results from the experiments validated the findings from the Response Surface Methodology (RSM), as shown in Table 3. The predicted compressive strength values closely matched the experimental results, confirming that RSM provides an accurate prediction of compressive strength. (He et al., 2016; Pandey and Kumar, 2019; Wang et al., 2021).

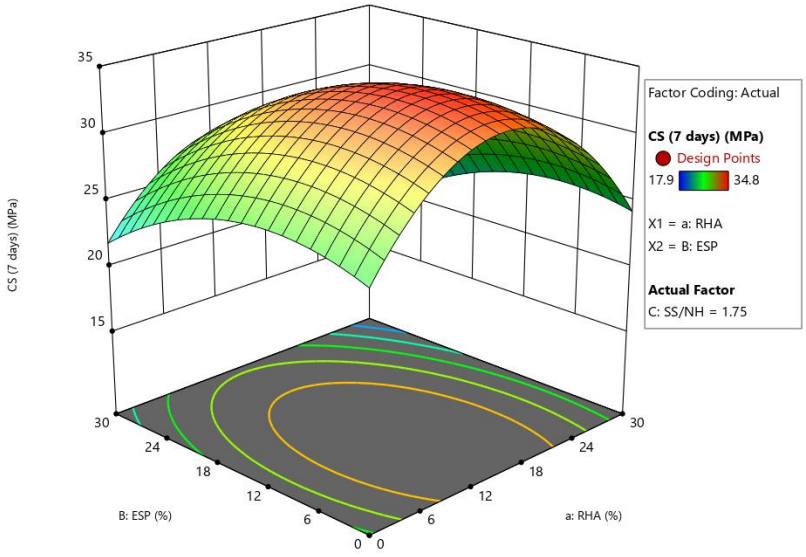

a)

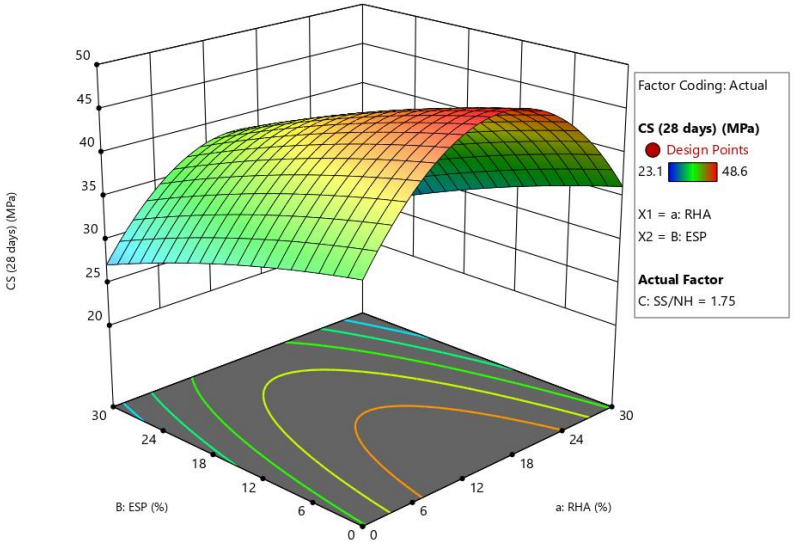

b)

Fig. 8. Compressive strength results of the prepared Mixtures

Table.2. Input and output Parameters of the prepared Mixtures using RSM

Name	Units	Type	Changes	Std. Dev.	Low	High
RHA	%	Factor	Hard	0	0	30
ESP	%	Factor	Easy	0	0	30
SS/NH		Factor	Easy	0	1	2.5
CS (7 days)	MPa	Response			17.9	34.8
CS (28 days)	MPa	Response			23.1	48.6

Table.3. Compressive strength results of the prepared Mixtures

Group	Run	Factor 1 a:RHA	Factor 2 B:ESP	Factor 3 C:SS/NH	Response 1 CS (7 days)	Response 2 CS (28 days)
		%	%		MPa	MPa
1	1	0	0	2.5	29.6	38.8
1	2	0	17.4	1.63169	26.3	31.2
1	3	0	30	2.5	22.1	26.5
1	4	0	0	1	22.9	27.8
2	5	30	9.9	1.03	24.6	33.6
2	6	30	29.55	1.9825	17.9	23.1
2	7	30	0	2.5	26.9	31
3	8	15	0.75	1.6975	33.2	48.6
3	9	15	16.05	2.47	34.8	41.33
3	10	15	30	1	29.6	37

3.3 Machine learning analysis

Fig. 9 presents the experimental results alongside the predictions from three ML models regarding the CS of geopolymer concrete. The predicted CS values closely matched the experimental data for both training and testing phases (Abdellatief et al., 2024b, 2024c; Xiao et al., 2021). Fig. 10 displays the residuals of CS results of three models. The results indicated that the GPR model achieve high percentage of accuracy to predict the CS of geopolymer concrete. Additionally, the average R^2 values for the GPR, ANN, and Extreme GB models were 0.97, 0.96, and 0.84, respectively, in the training set, and 0.84, 0.41, and 0.67 in the testing set. The GPR model exhibited the highest R^2, indicating its superior performance among the models evaluated as presented in Table 3. Consequently, the GPR model allows for accurate predictions of CS. In contrast, the ANN and GB models would require additional data and numerous experiments to achieve reliable predictions.

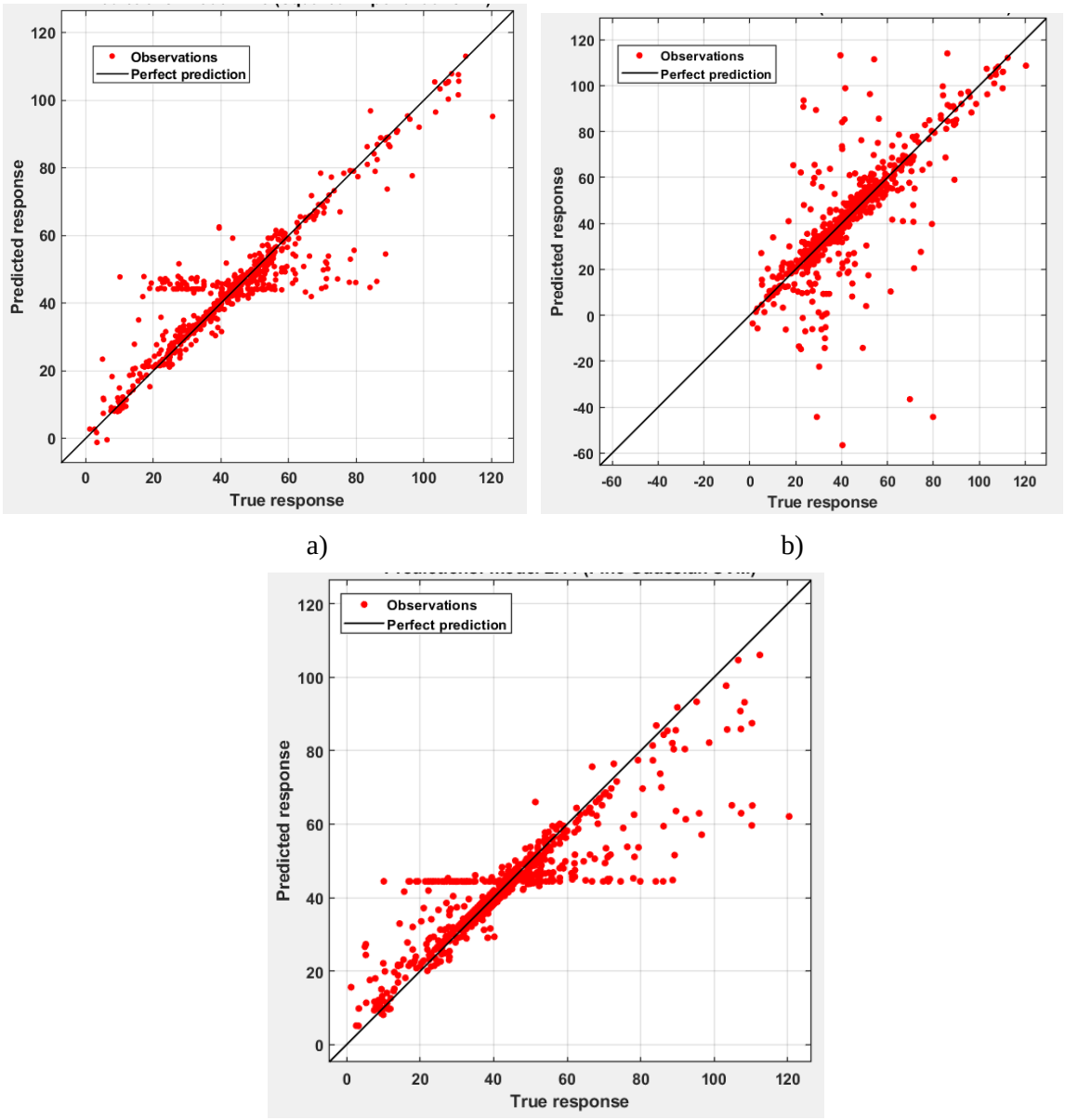

Fig. 9. Correlation diagrams of a) GPR, b) ANN, c) GB model

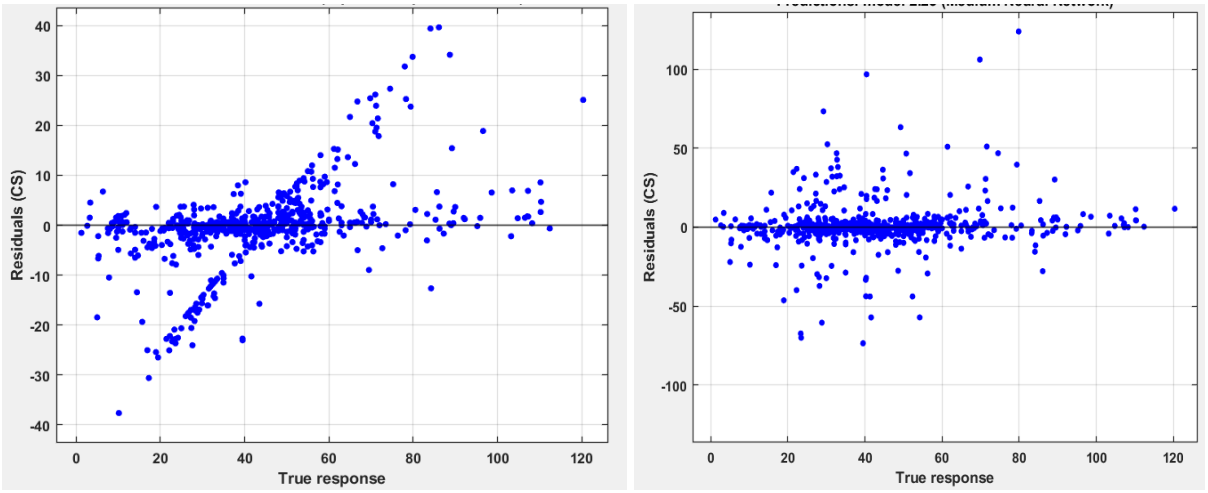

a) b)

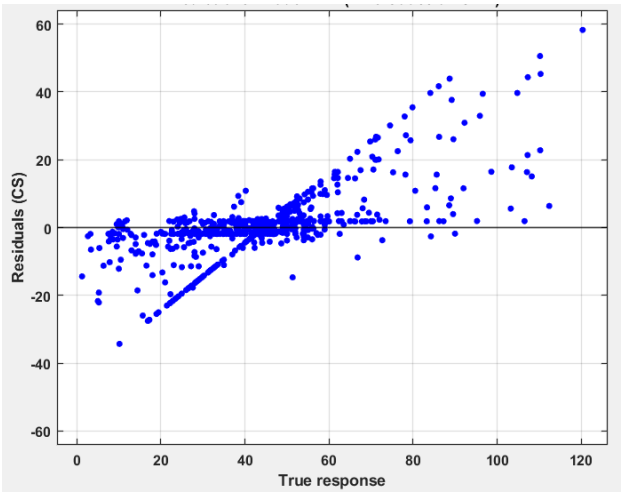

c)

Fig. 10. The residuals of CS of GM: a) GPR model, b) ANN model, and c) GB model.

Table 3. Best results of R^2, RMSE and MAE for three ML models

Models		Best		
		GPR	ANN	GB
R^2	Training	0.97	0.96	0.84
	Testing	0.84	0.41	0.67
MAE	Training	2.09	2.69	5.80
	Testing	4.69	7.70	7.79
RMSE	Training	3.65	4.16	8.44
	Testing	8.28	16.0	12.02

Fig. 11 illustrates the average relevance values of three models for each attribute, highlighting that the percentage of GGBS is the most critical factor influencing the CS predictions. This finding is consistent with previous experimental studies [47-49], which demonstrated that steel fibers significantly enhance the strength and microstructural properties of geopolymer. Among the models assessed, the GPR model exhibited the best performance, identifying the accurate sand and water content as the second and third most important features, respectively. While, the presence of coarse aggregate in geopolymer concrete contributes to a reducing the geopolymerization process, which ultimately decreases the material's CS strength and durability. Furthermore, the formation of geopolymer gel in concrete is greatly enhanced by a substantial presence of soluble silicates (such as NaOH and Na_2SiO_3) in alkali-activated concrete (R and A, 2020; Tiong et al., 2020; Xiao et al., 2020; Zhao and Li, 2022).

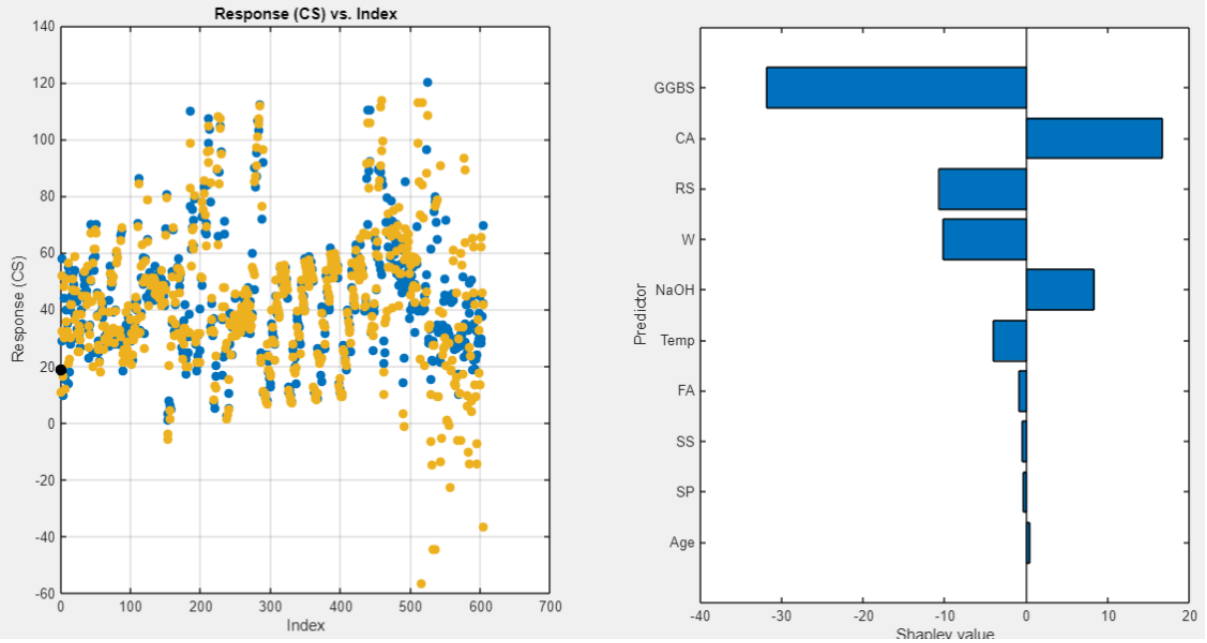

Fig. 11 The average relevance values of three models for each input parameter.

3.4 Ecological assessment of the HPGC Samples

Average estimates for the ecological assessment of the components used in the GM samples were gathered from the literature and are presented in Table 4. According to this table, NaOH, GGBFS, and SPs exhibit higher CO_2 emissions. The embodied energy (EE) and emission carbon (EC) values for the mixtures were calculated using data from credible sources, as detailed in Tables 5 and 6 (Abdellatief et al., 2023b, 2023c; Abd Ellatief et al., 2023).

Table 4. Inventory of cost, CE, and EE of used materials (Abd Ellatief et al., 2023; Gao et al., 2017; Hafez et al., 2021; Meng et al., 2019; Stengel and Schießl, 2014; Swathi and Vidjeapriya, 2023).

ID	Component	CE (kg/kg)	EE (MJ/kg)
1	GGBFS	0.019	1.588
3	ESP	0.88	0.02021
4	RHA	0.133	1.31
5	Fine aggregate	0.001	0.022
6	SP	0.22	11.5
7	Water	0.0002	0.01
8	NaOH	0.046	1.1148
9	Na_2SiO_3	1.213	0.000288

Fig. 13 illustrates the overall EC and EE of the prepared geopolymer mixtures. Notably, the control sample, which contains 30% RHA, showed the lowest EE (424.95 MJ/kg). The findings of this study suggest that using alternative precursor materials such as RHA can significantly reduce the environmental impact of geopolymer materials. However, it is important to acknowledge certain limitations, including challenges in generalizing results due to regional variations and the influence of selected functional units. Further exploration of the relationship between environmental performance and cost-effectiveness, along with advancements in production technologies, could enhance our understanding and promote sustainability in the construction industry.

Table 5. Calculated CE of prepared mixtures

Mixture ID	GGBFS	RHA		ESP	ESP	Sand	SS	NH	SP	Total CE
		%		%						kg/kg
M1	13.3	0	0	0	0	1.02	406.355	2.99	5.28	428.945
M2	10.982	0	0	17.5	2.91	1.02	406.355	2.99	5.28	429.537
M3	9.31	0	0	30	5.01	1.02	406.355	2.99	5.28	429.965
M4	11.97	0	0	10	1.65	1.02	406.355	2.99	5.28	429.265
M5	7.98	30	3.46	10	1.65	1.02	406.355	2.99	5.28	428.735
M6	5.32	30	553.6	30	4.92	1.02	406.355	2.99	5.28	979.485
M7	9.31	30	0	0	0	1.02	406.355	2.99	5.28	424.955
M8	11.21	15	38.28	1	0.15	1.02	406.355	2.99	5.28	465.285
M9	9.177	15	48.72	16	2.67	1.02	406.355	2.99	5.28	476.212
M10	7.315	15	0	30	5.01	1.02	406.355	2.99	5.28	427.97

Table 6. Calculated EE of prepared mixtures

Mixture ID	GGBFS	RHA %		ESP %	ESP	Sand	SS	NH	SP	Total CE kg/kg
M1	1111.6	0	0.00	0	0.000	22.440	0.096	72.462	276.000	1482.59
M2	10.98	0	0.00	17.5	1.960	22.440	0.096	72.462	276.000	383.941
M3	9.310	0	0.00	30	3.375	22.440	0.096	72.462	276.000	383.684
M4	11.970	0	0.00	10	1.112	22.440	0.096	72.462	276.000	384.080
M5	7.980	30	226.6	10	1.112	22.440	0.096	72.462	276.000	606.720
M6	5.320	30	226.6	30	3.314	22.440	0.096	72.462	276.000	606.263
M7	9.310	30	226.6	0	0.000	22.440	0.096	72.462	276.000	606.938
M8	11.210	15	113.9	1	0.101	22.440	0.096	72.462	276.000	496.280
M9	9.177	15	113.9	16	1.799	22.440	0.096	72.462	276.000	495.944
M10	7.315	15	113.9	30	3.375	22.440	0.096	72.462	276.000	495.659

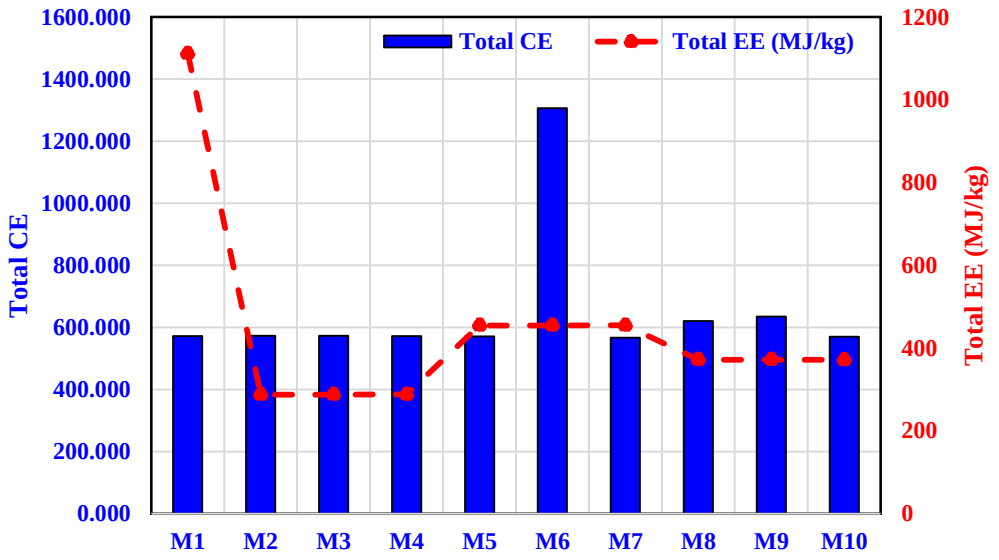

Fig. 13. Results of overall EC and EE of the prepared GM samples.

4. CONCLUSIONS

1. The use of RHA and ESP in geopolymer concrete promotes recycling and addresses ecological issues, contributing to sustainable construction practices.
2. Optimal incorporation of RHA and ESP significantly enhances the compressive strength of geopolymer concrete, with maximum strength reaching 48 MPa at specific ratios.
3. Response Surface Methodology (RSM) accurately predicts compressive strength based on varying dosages of RHA and ESP, validating the experimental results.
4. Among the machine learning models used, Gaussian Process Regression (GPR) exhibited the highest

accuracy in predicting compressive strength, highlighting the potential of advanced analytical techniques in material science.

5. The ecological assessment indicates that geopolymer concrete incorporating RHA and ESP results in lower CO_2 emissions, supporting environmental sustainability.
6. Further studies should focus on the long-term performance of geopolymer concrete with these materials and explore the relationship between environmental impact and cost-effectiveness.

5. References

Abd Ellatief, M., Abadel, A.A., Federowicz, K., Abd Elrahman, M., 2023. Mechanical properties, high temperature resistance and microstructure of eco-friendly ultra-high performance geopolymer concrete: Role of ceramic waste addition. Constr Build Mater 401, 132677. https://doi.org/https://doi.org/10.1016/j.conbuildmat.2023.132677

Abdellatief, M., Ahmed, Y.M., Taman, M., Elfadaly, E., Tang, Y., Abadel, A.A., 2024a. Physico-mechanical, thermal insulation properties, and microstructure of geopolymer foam concrete containing sawdust ash and egg shell. Journal of Building Engineering 90, 109374. https://doi.org/10.1016/J.JOBE.2024.109374

Abdellatief, M., Elrahman, M.A., Abadel, A.A., Wasim, M., Tahwia, A., 2023. Ultra-high performance concrete versus ultra-high performance geopolymer concrete: Mechanical performance, microstructure, and ecological assessment. Journal of Building Engineering 79, 107835. https://doi.org/10.1016/J.JOBE.2023.107835

Abdellatief, M., Hassan, Y.M., Elnabwy, M.T., Wong, L.S., Chin, R.J., Mo, K.H., 2024b. Investigation of machine learning models in predicting compressive strength for ultra-high-performance geopolymer concrete: A comparative study. Constr Build Mater 436, 136884. https://doi.org/https://doi.org/10.1016/j.conbuildmat.2024.136884

Abdellatief, M., Wong, L.S., Din, N.M., Mo, K.H., Ahmed, A.N., El-Shafie, A., 2024c. Evaluating enhanced predictive modeling of foam concrete compressive strength using artificial intelligence algorithms. Mater Today Commun 40, 110022. https://doi.org/https://doi.org/10.1016/j.mtcomm.2024.110022

Adamu, M., Alanazi, H., Ibrahim, Y.E., Abdellatief, M., 2024a. Mechanical, microstructural characteristics and sustainability analysis of concrete incorporating date palm ash and eggshell powder as ternary blends cementitious materials. Constr Build Mater 411, 134753. https://doi.org/10.1016/J.CONBUILDMAT.2023.134753

Adamu, M., Alanazi, H., Ibrahim, Y.E., Abdellatief, M., 2024b. Mechanical, microstructural characteristics and sustainability analysis of concrete incorporating date palm ash and eggshell powder as ternary blends cementitious materials. Constr Build Mater 411, 134753. https://doi.org/10.1016/J.CONBUILDMAT.2023.134753

Albidah, A., Alqarni, A.S., Abbas, H., Almusallam, T., Al-Salloum, Y., 2022. Behavior of Metakaolin-Based geopolymer concrete at ambient and elevated temperatures. Constr Build Mater 317, 125910. https://doi.org/https://doi.org/10.1016/j.conbuildmat.2021.125910

Cai, R., Wu, T., Fu, C., Ye, H., 2022. Thermal degradation of potassium-activated ternary slag-fly ash-silica fume binders. Constr Build Mater 320, 126304. https://doi.org/10.1016/J.CONBUILDMAT.2021.126304

Gao, X., Yu, Q.L., Yu, R., Brouwers, H.J.H., 2017. Evaluation of hybrid steel fiber reinforcement in high performance geopolymer composites. Mater Struct 50, 165. https://doi.org/10.1617/s11527-017-1030-x

Hafez, H., Kurda, R., Al-Ayish, N., Garcia-Segura, T., Cheung, W.M., Nagaratnam, B., 2021. A whole life cycle performance-based ECOnomic and ECOlogical assessment framework (ECO2) for concrete sustainability. J Clean Prod 292, 126060. https://doi.org/https://doi.org/10.1016/j.jclepro.2021.126060

He, P., Wang, M., Fu, S., Jia, D., Yan, S., Yuan, J., Xu, J., Wang, P., Zhou, Y., 2016. Effects of Si/Al ratio on the structure and properties of metakaolin based geopolymer. Ceram Int 42, 14416–14422. https://doi.org/https://doi.org/10.1016/j.ceramint.2016.06.033

Hesami, S., Ahmadi, S., Nematzadeh, M., 2014. Effects of rice husk ash and fiber on mechanical properties of pervious concrete pavement. Constr Build Mater 53, 680–691. https://doi.org/10.1016/J.CONBUILDMAT.2013.11.070

Ifzaznah, H.H.H., Güllü, A., Memiş, S., Yaprak, H., Gencel, O., Ozbakkaloglu, T., 2024. Performance, cost, and ecological assessment of fiber-reinforced high-performance mortar incorporating pumice powder and ground granulated blast furnace slag as partial cement replacement. J Clean Prod 476, 143720.

https://doi.org/https://doi.org/10.1016/j.jclepro.2024.143720

Liu, J., Doh, J.-H., Dinh, H.L., Ong, D.E.L., Zi, G., You, I., 2022. Effect of Si/Al molar ratio on the strength behavior of geopolymer derived from various industrial waste: A current state of the art review. Constr Build Mater 329, 127134. https://doi.org/https://doi.org/10.1016/j.conbuildmat.2022.127134

Meng, Q., Wu, C., Su, Y., Li, J., Liu, J., Pang, J., 2019. Experimental and numerical investigation of blast resistant capacity of high performance geopolymer concrete panels. Compos B Eng 171, 9–19. https://doi.org/https://doi.org/10.1016/j.compositesb.2019.04.010

Pandey, A., Kumar, B., 2019. Effects of rice straw ash and micro silica on mechanical properties of pavement quality concrete. Journal of Building Engineering 26, 100889. https://doi.org/https://doi.org/10.1016/j.jobe.2019.100889

Paruthi, S., Khan, A.H., Kumar, A., Kumar, F., Hasan, M.A., Magbool, H.M., Manzar, M.S., 2023. Sustainable cement replacement using waste eggshells: A review on mechanical properties of eggshell concrete and strength prediction using artificial neural network. Case Studies in Construction Materials 18, e02160. https://doi.org/10.1016/J.CSCM.2023.E02160

R, C.P., A, M.S., 2020. Quantitative Assessment of Alkali-Activated Materials: Environmental Impact and Property Assessments. Journal of Infrastructure Systems 26, 04020021. https://doi.org/10.1061/(ASCE)IS.1943-555X.0000556

Shah, S.N., Mo, K.H., Yap, S.P., Radwan, M.K.H., 2021. Towards an energy efficient cement composite incorporating silica aerogel: A state of the art review. Journal of Building Engineering 44, 103227. https://doi.org/10.1016/J.JOBE.2021.103227

Stengel, T., Schießl, P., 2014. 22 - Life cycle assessment (LCA) of ultra high performance concrete (UHPC) structures, in: Pacheco-Torgal, F., Cabeza, L.F., Labrincha, J., de Magalhães, A. (Eds.), Eco-Efficient Construction and Building Materials. Woodhead Publishing, pp. 528–564. https://doi.org/https://doi.org/10.1533/9780857097729.3.528

Swathi, B., Vidjeapriya, R., 2023. Influence of precursor materials and molar ratios on normal, high, and ultra-high performance geopolymer concrete – A state of art review. Constr Build Mater 392, 132006. https://doi.org/https://doi.org/10.1016/j.conbuildmat.2023.132006

Tahwia, Ahmed M, Aldulaimi, D.S., Abdellatief, M., Youssf, O., 2024. Physical, Mechanical and Durability Properties of Eco-Friendly Engineered Geopolymer Composites. Infrastructures (Basel) 9. https://doi.org/10.3390/infrastructures9110191

Tahwia, A.M., Ellatief, M.A., Bassioni, G., Heniegal, A.M., Elrahman, M.A., 2023. Influence of high temperature exposure on compressive strength and microstructure of ultra-high performance geopolymer concrete with waste glass and ceramic. Journal of Materials Research and Technology 23, 5681–5697. https://doi.org/10.1016/J.JMRT.2023.02.177

Tahwia, Ahmed M., Elmansy, A. k., Abdellatief, M., Elrahman, M.A., 2024. Durability and ecological assessment of low-carbon high-strength concrete with short AR-glass fibers: Effects of high-volume of solid waste materials. Constr Build Mater 429, 136422. https://doi.org/10.1016/J.CONBUILDMAT.2024.136422

Tiong, H.Y., Lim, S.K., Lee, Y.L., Ong, C.F., Yew, M.K., 2020. Environmental impact and quality assessment of using eggshell powder incorporated in lightweight foamed concrete. Constr Build Mater 244, 118341. https://doi.org/10.1016/J.CONBUILDMAT.2020.118341

Wang, S., Song, X., Wei, M., Liu, W., Wang, X., Ke, Y., Tao, T., 2021. Strength characteristics and microstructure evolution of cemented tailings backfill with rice straw ash as an alternative binder. Constr Build Mater 297, 123780. https://doi.org/https://doi.org/10.1016/j.conbuildmat.2021.123780

Xiao, R., Ma, Y., Jiang, X., Zhang, M., Zhang, Y., Wang, Y., Huang, B., He, Q., 2020. Strength, microstructure, efflorescence behavior and environmental impacts of waste glass geopolymers cured at ambient temperature. J Clean Prod 252, 119610. https://doi.org/10.1016/J.JCLEPRO.2019.119610

Xiao, R., Zhang, Y., Jiang, X., Polaczyk, P., Ma, Y., Huang, B., 2021. Alkali-activated slag supplemented with waste glass powder: Laboratory characterization, thermodynamic modelling and sustainability analysis. J Clean Prod 286, 125554. https://doi.org/10.1016/J.JCLEPRO.2020.125554

Zhao, J., Li, S., 2022. Performance study and environmental evaluation of alkali-activated materials based on waste photovoltaic glass. J Clean Prod 379, 134576. https://doi.org/10.1016/J.JCLEPRO.2022.134576